Title
Ammonia as a Contaminant in the Performance of an Integrated SOFC Reformer System

ISBN
9780791837801

Authors
Yi, Yaofan
Rao, Ashok
Brouwer, Jacob
et al.

Publication Date
2006

DOI
10.1115/fuelcell2006-97037

Proceedings of FUELCELL2006
The 4th International Conference on FUEL CELL SCIENCE, ENGINEERING and TECHNOLOGY
June 19-21, 2006, Irvine, CA

FUELCELL2006-97037

AMMONIA AS A CONTAMINANT IN THE PERFORMANCE OF AN INTEGRATED SOFC REFORMER SYSTEM

Yaofan Yi Ashok Rao Jacob Brouwer Scott Samuelsen

National Fuel Cell Research Center (NFCRC), University of California,
Irvine, CA 92697-3550, USA

ABSTRACT

As supply of natural gas (NG) is limited, more attention is being given to operating fuel cells on syngas derived from gasification of feedstocks such as coal and biomass. Ammonia (NH_3) is one of the problematic contaminants contained in syngas produced from these nitrogen containing feedstocks. NH_3 can be easily oxidized to nitric oxide (NO) in a combustion process and thus if present in the anode exhaust gas would be problematic. The potential effects of NH_3 (particularly at low levels) on fuel cell system performance have not been well studied. The former studies on NH_3 have been limited to either the reforming process alone or testing the fuel cell at the cell level with NH_3 containing gases. No studies have been accomplished on a fuel cell system level basis. Objectives of this work are to obtain a comprehensive understanding of fuel cell system performance on syngas containing NH_3 using an integrated SOFC reformer system. Detailed analysis is conducted within the three major reacting components – indirect internal reformer, SOFC stack and combustion zone. Various simulation tools (etc., CHEMKIN, ASPEN, APSAT) are utilized for analysis. Results show that NH_3 conversion (into N_2 and H_2) in the internal reformer is about 50% when temperature is 750°C. NH_3 conversion (into N_2 and H_2) in the SOFC stack can affect NO_x emissions significantly. More than 50% NH_3 left from SOFC stack can convert into NO_x in the combustion zone. Experimental study is also planned to validate the theoretical results.

Keywords: Ammonia (NH_3); Impurity; Nitrogen oxides (NO_x); Solid Oxide Fuel Cell (SOFC); Coal syngas (CS)

1. INTRODUCTION

It is well recognized that solid oxide fuel cell has a significant advantage of fuel flexibility over the low temperature fuel cells [1]. Various fuels can be processed to produce a reformate (containing primarily H_2 and CO) for direct use in a solid oxide fuel cell. The main fuel sources used to produce this reformate include fossil fuels (e.g., natural gas, oil and coal), and renewable fuels (e.g., biomass and waste). The impacts of multi-fuel operation of integrated SOFC reformer systems on component performance, design point selection, thermal management and overall system efficiency were discussed [2]. However, the potential effects of one major fuel impurity – NH_3, haven't been studied well.

Depending on the gasifier design, operating conditions and the fuel bound N_2 content, the concentration of NH_3 in the coal syngas can be as high as 0.5 mol% [3-7]. Water based NH_3 removal systems involve cooling the syngas to around 400K, and can remove a substantial amount of NH_3, with residual levels of up to 400ppm as reported [4]. Although the sensible heat recovered in this cooling process may be effectively utilized elsewhere, the process results in reduced cycle efficiency and is not preferable in the advanced power generation design. High temperature clean up systems, which can provide higher efficiency and have less serious tar issues, however remove very little or no NH_3 at all [4, 8].

In the state-of-the-art integrated coal gasification, high temperature fuel cell and gas turbine hybrid systems, NH_3 contained in the cleaned coal gas is first passed through fuel cell before entering gas turbine. Any remaining NH_3 after the fuel cell stack may be converted to nitrogen oxides in the gas turbine combustor. Understanding of NH_3 performance in the

SOFC system is thus important for coal based SOFC hybrid systems.

In addition to being present in coal derived syngas, NH_3 is also present in gas derived from pyrolysis of nitrogen bearing feedstocks such as biomass [8, 13].

Recently, a number of research groups [9-12] have been showing great interest in NH_3 as a H_2 carrier or a direct fuel for fuel cells, which are, however, beyond the current scope of this study.

The former studies on NH_3 conversion are limited to either reforming processes or the fuel cell [10, 12-15] but none on a system level basis. Very little litereature work can be found to have detailed study on NH_3 reaction at very low partial pressure (<2.6 torr) in the reformer. Objectives of this work are to theoretically study the performance of low content NH_3 within a pre-commercial integrated SOFC system. Detailed study will be conducted within the three major components – reformer, SOFC stack and combustion zone. In the further step, strategies on NO_x emissions control within integrated coal gasification, fuel cell and gas turbine combined cycle will be proposed. Experimental study is also planned based on the theoretical results.

2. SOFC SYSTEM DESCRIPTION

A typical integrated SOFC reformer system, the Siemens Westinghouse 25 kW SOFC system [2], is studied in this work. Figure 1 presents an overall system schematic and details of the SOFC stack design based on natural gas fuel. Compressed and desulfurized natural gas is fed to indirect internal reformers (or pre-reformers) with part of spent fuel from an anode off-gas recirculation plenum near the top of the fuel cell stack. In the nickel-based reformers, methane (CH_4) or any higher hydrocarbons react with the steam brought with spent fuel at a temperature as high as 750°C, and are converted to H_2, CO, CO_2, and remaining CH_4. This reformed fuel mixture then enters a fuel manifold at the bottom of the stack where it flows upwards and is distributed to the outside surface of the tubular cells. Meanwhile, after preheating in a recuperator, air is fed by an injection tube and flows upwards along the inside surface of the tubular cells. With fuel on the outside and oxygen from the air on the inside electrochemical reactions take place along the length of the cells. The temperature inside the module and along the length of each cell varies somewhat but the maximum temperature is generally kept below 980°C – 1050°C. Anode off-gas enters the recirculation plenum where a fraction of it is recirculated and the balance flows into the combustion plenum to mix with the depleted air. The small amount of remaining anode off-gas is combusted with the depleted air to preheat the air through the recuperator and provide heat to the reformers before it is exhausted. Notice that Figure 1 just presents the overall concept for stack design. More details about mixing phenomena for combustion zone will be described and discussed in the following modeling section.

The main interest of this work is to investigate the performance of NH_3 as an impurity within the integrated SOFC system, which contains three major components where NH_3 reactions can occur: the reformer, SOFC stack and combustor. The process flow diagram among those three reactors is shown in Figure 2. The detailed configuration of each component will be described in the following sections. Other components, such as recuperator and heater, are not presented in this diagram.

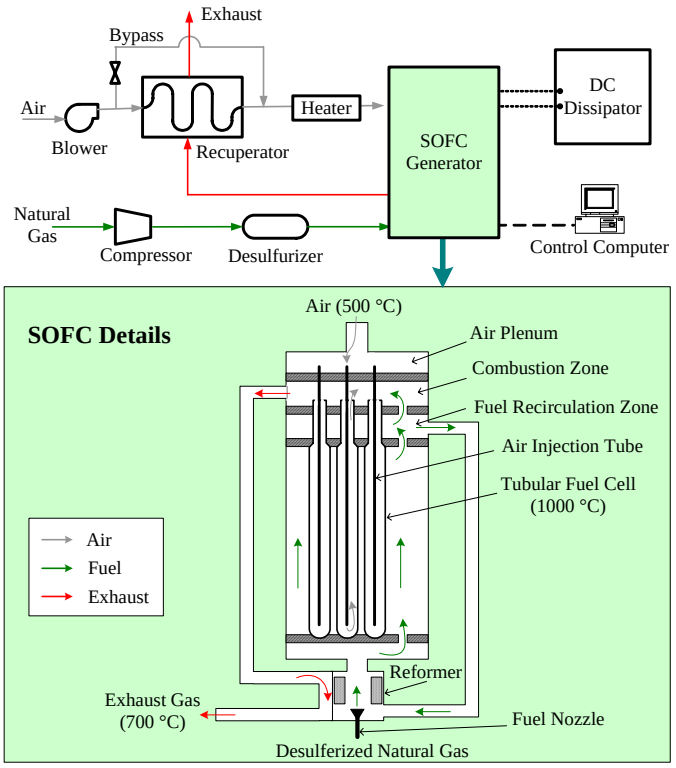

Figure 1: System schematic and SOFC module details of the Siemens Westinghouse 25 kW SOFC system [2]

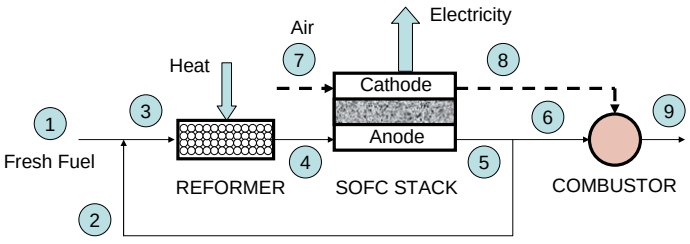

1. Fresh Fuel	4. Anode Inlet Fuel	7. Cathode Inlet Air
2. Recycled Fuel	5. Depleted Fuel	8. Cathode Outlet
3. Mixed Fuel Stream	6. Fuel to Combustor	9. Combustor Exhaust

Figure 2: Process diagram for SOFC with anode recycle

3. NH_3 REACTION MECHANISMS

3.1. Reformer

Four identical reformers with nickel based catalyst are used within 25kW SOFC system, each per quadrant of SOFC stack. Operating temperature is maintained within the range of 720-750°C. The reformer annular geometry (see Figure 3) is: inside radius r_{in} = 6.6 cm, outside radius r_{out} = 8.4 cm, length L = 40 cm.

Based on the previous studies [14, 16-21], the working conditions within 25kW SOFC internal reformer consisting of high temperature (up to 750°C), low pressure (~1.1 bar), and presence of nickel-based catalyst used for steam reformation, can promote the decomposition of NH_3 via the following overall endothermic reaction:

$$2NH_3 \rightarrow N_2 + 3H_2 \qquad H = 11 \ kcal/mol \tag{1}$$

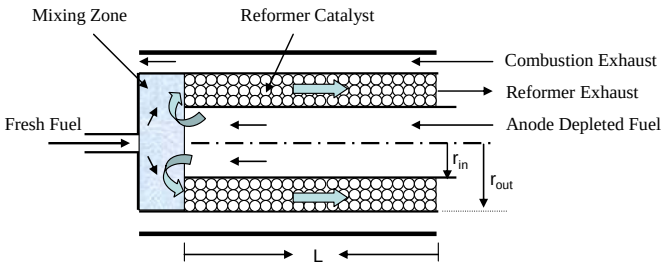

Figure 3: Reformer geometry and internal flow configuration

Commercial NH_3 cracking units are designed based on the above reaction mechanism to produce mixture of H_2 and N_2 from anhydrous NH_3. When reaction takes place on nickel catalyst at a temperature of 850°C to 900°C, most of the NH_3 is cracked and residual NH_3 content is rather low, less than 100ppm without requiring additional purifier as reported [18, 22].

Due to the lower reaction temperature and much lower NH_3 concentration compared to the commercial NH_3 cracking units, however, the internal reformer might not convert most of the NH_3 into H_2 and N_2 before it enters the SOFC stack. Quantitative assessment of residual NH_3 level in the reformer outlet requires a further understanding of NH_3 decomposition mechanism under the reaction conditions unique to the reformer.

In this work, NH_3 contained in the fuel is at impurity level of less than 0.5% by volume. At low NH_3 concentrations, reaction mechanism for NH_3 decomposition can be described using the following sequence [10, 23]:

Step 1: $NH_3 \xleftrightarrow{k_1} NH_3(ad)$ (2)

Step 2: $NH_3(ad) \xrightarrow{k_2} NH_2(ad) + H(ad)$ (3)

Step 3: $NH_2(ad) \xrightarrow{k_3} NH(ad) + H(ad)$ (4)

Step 4: $NH(ad) + H(ad) \xrightarrow{k_4} N(ad) + 3H(ad)$ (5)

Step 5: $2H(ad) \xrightarrow{k_5} H_2$ (6)

Step 6: $2N(ad) \xrightarrow{k_6} N_2$ (7)

where (ad) denotes that the species is adsorbed on the catalyst surface.

Depending on the reaction temperature, rate limiting step in catalytic NH_3 decomposition can be the NH_3 adsorption (1), the recombinative desorption of N_2 (step 6), or both. Step 2-5 are found kinetically insignificant [17, 19, 23].

a) Low Operating Temperature

When the temperature is low (<727°C based on nickel catalyst), the decomposition rate is independent of NH_3 partial pressure, where the rate-limiting step is the recombinative desorption of N_2, with activation energies around 125-210 kJ/mol [19, 21]. The NH_3 decomposition rate is closely approximated by [21]:

$$r_{NH_3} = n_0 \cdot k_6 \tag{8}$$

where, n_0 is the nickel surface atom density and is given as $1.5 \times 10^{15} cm^{-2}$; k_6 is the rate constant for the N_2 recombination in step 6, and is given as [21]:

$$k_6 = 1 \times 10^{13} s^{-1} \cdot \exp\left(\frac{-211 kJ \cdot mol^{-1}}{RT}\right) \tag{9}$$

b) High Operating Temperature

When the temperature is high (>727°C based on nickel catalyst), the decomposition rate is first-order dependent on NH_3 partial pressure and the rate-limiting step is the NH_3 adsorption, with activation energies in the range of 16-42 kJ/mol [19, 21]. When partial pressure of NH_3 is low, the decomposition rate is independent of N_2 and H_2 partial pressures [19, 24].

Based on the above observations, a power law rate model was suggested [19, 21] to express the NH_3 decomposition rate at high temperature and low NH_3 partial pressure:

$$r_{NH_3} = k_1 \cdot p_{NH_3} \tag{10}$$

where, k_1 is rate constant for NH_3 adsorption in the step 1 of NH_3 decomposition, and p is the partial pressure. k_1 is given as [21]:

$$k_1 = 4.07 \times 10^{16} molecules \cdot cm^{-2} \cdot s^{-1} \cdot Pa^{-1} \tag{11}$$

At temperature higher than 520°C, rate constant was obtained to fit experimental data for NH_3 decomposition using a nickel based catalyst [19]:

$$k_1 = 1.309 \times 10^{12} \cdot \exp\left(\frac{-2.06 \times 10^5 kJ \cdot mol^{-1}}{RT}\right) \tag{12}$$

In this work, NH_3 partial pressure is less than 2.6 torr (0.05 psi). The reformer operates at a temperature range of 720°C-750°C, within the high temperature region as discussed before. Therefore, NH_3 conversion can be regarded as dominated by NH_3 adsorption (step 1).

Other than expressed as a series of elementary reactions, surface reactions are also described and studied using global reactions. To seek a simple global rate expression, kinetics of

NH_3 decomposition on Ni/Al_2O_3 catalysts are described using the Temkin-Pyzhev mechanism [25-27]:

$$r_{NH_3} = k_0 \cdot \exp\left(\frac{-E}{RT}\right) \cdot \left(\frac{p_{N_2}}{K_{eq}^2} \left(\frac{p_{H_2}^3}{p_{NH_3}^2} \right)^{1-\beta} - \left(\frac{p_{NH_3}^2}{p_{H_2}^3} \right)^{\beta} \right) \quad (13)$$

where, K_{eq} is the thermodynamic equilibrium constant defined as:

$$\log(K_{eq}) = -\frac{2250.322}{T} + 0.85340 + 1.51049 \log T + 25.8987 \times 10^{-5} T - 14.8961 \times 10^{-8} T^2$$

Kinetic parameters, the pre-exponential factor k_0, the activation energy E and exponent constant β are measured experimentally in the pressure range 9-36 bar and a temperature range of 400-550°C [28]:

$k_0 = 5.744 \times 10^{19} \quad mol/(m^3 \cdot s \cdot Pa^{-0.674})$

$E = 2.304 \times 10^2 \quad kJ/mol$

$\beta = 0.674$

Kinetics of NH_3 decomposition on various catalysts, vanadium nitride (VN), palladium (Pd) and Iridium (Ir), have also been studied and expressed in Langmuir-Hinshelwood format [29-31].

However, none of the global rate expressions was found appropriate for reaction conditions of interest in this work, very low pressure and relatively high temperature (~750°C).

3.2. SOFC

All the NH_3 remained after the reformer will enter SOFC stack. Or, if a SOFC system is designed to operate directly on coal syngas without external or internal reformers, then the NH_3 contained in the coal syngas will be a potential concern for SOFC stack, either degrade the SOFC performance or generate nitrogen oxides (NO_x).

NH_3 as a fuel contaminant in coal syngas or biogas has been tested on SOFCs and showed no strong association of cell degradation [13, 32]. Instead, NH_3 has been considered as a direct fuel for fuel cell based on the reaction (18). In 1980, Farr at al. [12, 15] constructed and tested a solid electrolyte fuel cell operating on NH_3 fuel to generate electric energy and nitric oxide (NO for the production of HNO_3). It was shown that the fuel cell, [NH_3, NO, N_2, Pt/ZrO_2 (8% Y_2O_3)/Pt, air], produced mainly NO when operating at temperature around 1100K, and showed that Pt based catalyst has high selectivity to convert NH_3 into NO via electrochemical oxidation. Instead of producing NO, more recent research efforts are to avoid the NO formation in SOFC. The more recent concept for using NH_3 as a direct fuel in SOFC is sending NH_3 directly to SOFC anode surface containing a catalyst, such as iron oxide, Fe_2O_3, or nickel-based compound. NH_3 is first cracked into N_2 and H_2, and the generated H_2 is then utilized for the electrochemical generation of electricity. Based on the experimental results using silver anode and platinum anode with or without iron-based catalyst, Wojcik et al. [14] predicted that NH_3 could work very well in an SOFC system based on nickel anodes, although no actual experimental work has been conducted on nickel anode SOFC in their work. NH_3 performance in a SOFC with Ni/8YSZ anode was studied by Dekker et al. [10]. In their cell tests, the fuel cell outlet gas was measured and analyzed for NO_x and NH_3 to determine the NH_3 conversion. It was concluded that at operating temperature of 800-1000°C, the conversion of NH_3 is higher than 99.996% due to the withdrawal of H_2 by the electrochemical reaction and is close to the thermodynamic equilibrium. Most of the NH_3 is cracked into H_2 and N_2. The NO_x outlet concentration of the fuel cell was measured to be below 0.5 ppm at temperature up to 950°C and around 4 ppm at 1000°C.

Some researchers [10, 13] argue that NH_3 as a fuel or fuel impurity can be completely converted into N_2 and H_2 over the SOFC nickel based anode when temperature is high (> 590°C as found in [13]). However, other research groups [19, 21] found out that NH_3 conversion on nickel based catalyst can be high but never reach an equilibrium level even with nickel based catalyst and within high temperature range (>500°C). For example, NH_3 conversion on Ni-Pt/Al2O3 catalyst was measured higher than 80% but less than 99% in the temperature range of 520-690°C [19]. From theoretical understanding, high operating temperature of SOFC helps increase reaction rate, however, the overall limiting step for NH_3 conversion can be the mass transfer. Slow NH_3 diffusion especially at low concentration can limit the reach of NH_3 to catalyst surface and therefore leads to lower conversion. Moreover, H_2 existing at anode site, with much higher concentration and diffusivity compared to NH_3, can compete with NH_3 to reach catalyst surface, and further limit NH_3 conversion. Therefore, an accurate prediction of NH_3 conversion within SOFC stack should cover the effects of various factors including catalyst, temperature, residence time and fuel composition, especially, H_2 concentration and NH_3 concentration.

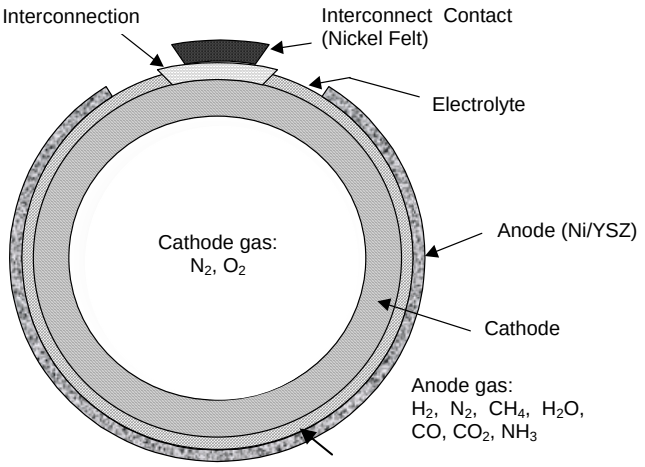

Figure 4: Cross-sections of a SOFC tube

SOFC anode side (fuel gas and anode surface) in this study contains the following species: H_2, CO, CO_2, H_2O, N_2, CH_4, NH_3 and O^{2-}. It is noteworthy that nickel, an active catalyst for NH_3 cracking as introduced before, is contained in both anode and interconnection contact, as shown in Figure 4 [33].

In the typical SOFC system operating on natural gas, anode reactions are generalized as:

$$H_2 + O^{2-} \rightarrow H_2O + 2e^- \quad (14)$$

$$CO + O^{2-} \rightarrow CO_2 + 2e^- \quad (15)$$

$$CH_4 + 4O^{2-} \rightarrow CO_2 + 2H_2O + 8e^- \quad (16)$$

Due to the existence of NH_3 and nickel catalyst, the following additional anode reactions are considered based on the suggestions by different studies [10, 12, 14, 15]:

a. NH_3 cracking:

$$2NH_3 \rightarrow N_2 + 3H_2 \quad (1)$$

b. Electrochemical reaction:

$$2NH_3 + 5O^{2-} \rightarrow 2NO + 3H_2O + 10e^- \quad (17)$$

c: NH_3 reduction via NO:

$$4NH_3 + 6NO \rightarrow 5N_2 + 6H_2O \quad (18)$$

Selectivity to NO or N_2 for NH_3 reaction depends on: catalyst, temperature, O^{2-} diffusivity and NH_3 diffusivity, residence time and NH_3 molar flow rate (content and total fuel flow rate). Within the temperature range of 700-1000°C, it was observed [34] that NO formation reaction (17) is selective with platinum based catalyst. NH_3 cracking reaction (1) is selective with nickel based catalyst.

Since none of the test results show that NH_3 would degrade SOFC performance, the only concern about NH_3 in SOFC stack is its possible causes for NO_x generation. No report has been found showing that significant amount of NO_x can be produced within fuel cell stack itself. Instead, NO_x may be produced when the depleted fuel cell anode gas containing NH_3 is combusted in a combustor before entering turbine. Theoretical study and experimental work are needed to determine the significance of NH_3 content within anode depleted gas on NO_x production or reduction (reaction (17) or (18)).

3.3. Combustion zone

Geometry and internal flow pattern of combustion zone are depicted in Figure 5 based on the schematics of the 25kW SOFC system provided by Siemens Westinghouse Power Corporation [33, 35], though the exact configuration and dimensions were not well known. The zone outlets were assumed to be through the sides of the zone (as shown in Figure 1), based on knowledge of the unit. Combustion zone outlet temperature is observed about 860°C, where the anode depleted fuel meet with cathode depleted gas (~16% O_2) and combust to generate heat. NH_3 at that temperature range can react to generate various products (etc., N_2, NO, N_2O) as discovered in various studies [36, 37].

No catalysts are utilized within the combustion zones. Therefore, the study focuses on non-catalytic reaction of NH_3. Actually, NH_3 is commonly used as a reducing agent for NO in both selective catalytic reduction (SCR) and selective non-catalytic reduction (SNCR). It was found that when NH_3 is injected into a fuel-lean zone, which is the case in this work, NO is reduced by the reactions (18) and (19) [37]:

$$4NH_3 + 4NO + O_2 \rightarrow 4N_2 + 6H_2O \quad (19)$$

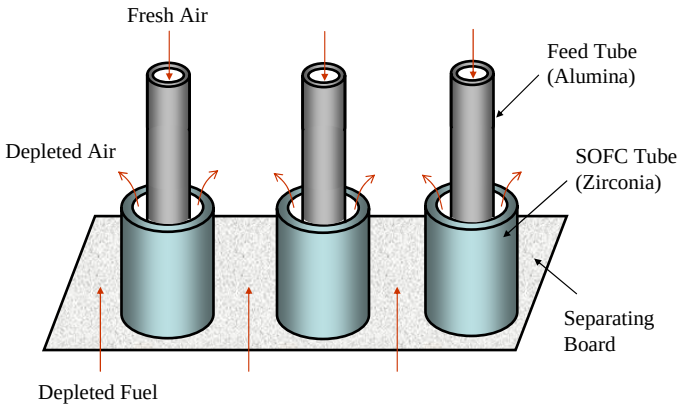

Figure 5: Schematic diagram of combustion zone

It was also reported that NH_3 gives effective reduction of NO emission within a narrow temperature window around 750-850°C. Average temperature (~860°C) of combustion zones studied in this work is slightly out of the temperature range. One negative effect is that if NH_3 is excess, NO and N_2O can be formed via the following overall reactions:

$$4NH_3 + 5O_2 \rightarrow 4NO + 6H_2O \quad (20)$$

$$4NH_3 + 4O_2 \rightarrow 2N_2O + 6H_2O \quad (21)$$

4. MODELING

4.1. Overall strategy and tools

ASPEN PLUS, a widely used commercial simulation tool for process engineering, is applied to determine the reaction kinetics within the reformer. ASPEN PLUS enables the users to define detailed reaction mechanisms and reactor conditions to predict reaction conversions, and understand reaction behavior. Detailed reformer model will be described in the later sections.

Reactions within SOFC stack are studied in two steps using two analysis tools:

1. Major reactions and products from SOFC stack, except those associated with NH_3 kinetics, are determined using a validated simulation tool – Advanced Power Systems Analysis Tool (APSAT). Details about APSAT and SOFC model can be seen in [38, 39].
2. As mentioned before, NH_3 decomposition under SOFC reaction conditions can be from 80% to 99.996%. Detailed model on NH_3 reaction and conversion is not investigated

in this work. Instead, different conversion levels are considered.

A model comprised of a series of perfectly stirred reactors (PSR) and a plug flow reactor (PFR) from CHEMKIN 4.0.2 is built for simulating the combustion zone.

4.2. Reformer

4.2.1 Reactor model setup

Geometry description and flow configuration of the annular steam reformer are shown in Figure 3. The detailed parameters and specifications are listed in Table 1. Reformer geometry was determined from the observed data [33, 40, 41], while the catalyst information was assumed based on the reference work [42]. The reformer is simulated as a plug flow reactor using RPlug model provided by APSEN PLUS (see Figure 6).

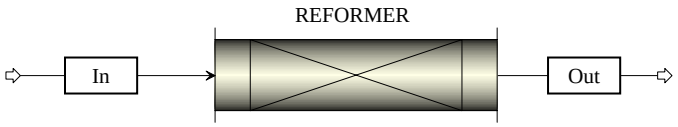

Figure 6: Reformer model setup (ASPEN RPlug)

Table 1: Reformer Description

Parameter	Value	Description
r_{in}	6.6 cm	Inside radius of reformer can
r_{out}	8.4 cm	Outside radius of reformer can
L	0.4 m	Length of reformer
ρ_c	2355 kg/m^3	Bulk density of catalyst
ε	0.528	Catalyst bed void fraction
α	9.3 m^2/gcat	Catalyst surface area per unit of mass

Table 2: Reformer operating conditions

Parameter	Natural gas	Coal syngas
Fresh fuel flow rate, g/s	0.211	1.21
Reformer inlet flow rate, g/s	1.262	1.54
NH_3 content in fresh fuel, %	0.2	0.2
Operation temperature, °C	750	750
Pressure, bar	1.14	1.14

Reformer operating conditions and flow information based on both cases of natural gas and coal syngas are summarized in Table 2. Constant operating pressure and temperature are assumed to approximate the actual steady-state operating conditions. A typical NH_3 content of 0.2% was assumed based on the reference work [3-7]. Coal syngas fresh fuel flow rate is much higher than natural gas due to its lower fuel heat value. Anode recirculation ratio is 0.55 for natural gas case and 0.15 for coal syngas. Those design details can be seen in the former work [2].

4.2.2 Reaction kinetics

Reaction mechanisms and rate expressions for NH_3 decomposition within reformer were discussed in the former section. Global reaction (1) is incorporated into the ASPEN PLUS model, and different reaction rate expressions are considered and compared.

Due to the low content of NH_3 existing in the reformer, NH_3 decomposition is interesting, however, not a dominating reaction. A complete model of reformer need include all the other possible reactions. Major reactions over a nickel supported catalyst within a steam reformer were widely adopted as a three-step mechanism:

1. Endothermic steam reforming reaction,

$$CH_4 + H_2O \leftrightarrow CO + 3H_2 \tag{22}$$

2. Exothermic water gas shift reaction,

$$CO + H_2O \leftrightarrow CO_2 + H_2 \tag{23}$$

3. Endothermic full steam reforming plus shift reaction,

$$CH_4 + 2H_2O \leftrightarrow CO_2 + 4H_2 \tag{24}$$

Langmuir–Hinshelwood mechanism, a mechanism for surface catalysis in which the reaction occurs between species that are adsorbed on the surface, is commonly applied to determine the reaction rates [26, 42-44]. Typical kinetic rate equations for steam reforming of methane are derived by Xu and Froment, whose work was carried out over a commercial catalyst ($Ni/MgAl_2O_4$, 15.2% nickel) [42, 43]:

$$r_1 = k_1\left(\frac{p_{CH_4}p_{H_2O}}{p_{H_2}^{2.5}} - \frac{p_{CO}p_{H_2}^{0.5}}{K_{p1}}\right)/DEN^2 \tag{25}$$

$$r_2 = k_2\left(\frac{p_{CO}p_{H_2O}}{p_{H_2}} - \frac{p_{CO_2}}{K_{p2}}\right)/DEN^2 \tag{26}$$

$$r_3 = k_3\left(\frac{p_{CH_4}p_{H_2O}^2}{p_{H_2}^{3.5}} - \frac{p_{CO_2}p_{H_2}^{0.5}}{K_{p3}}\right)/DEN^2 \tag{27}$$

$$DEN = 1 + K_{co}p_{co} + K_{H_2}p_{CH_4} + \frac{K_{H_2O}p_{H_2O}}{p_{H_2}} \tag{28}$$

where, p is partial pressure of each species in the reactor; r_1, r_2, r_3 stand for reaction rates for reactions (25), (26) and (27); k_1, k_2, k_3 are kinetic factors for each reaction; K_{p1}, K_{p2}, K_{p3} are equilibrium constants; K as shown in '*DEN*' term is adsorption constant for each species.

Kinetic factors k_1, k_2, k_3 and adsorption constants K_i are defined in Arrhenius format:

$$k_i = A_i \cdot \exp(-E_i / RT) \quad (29)$$

$$K_i = A_i \cdot \exp(-\Delta H_i / RT) \quad (30)$$

Table 3: Activation energy and pre-exponential factors for kinetic factors k_i

Kinetic factors	Activation energy E_i (kJ/mol)	Pre-exponential factor A_i
k_1	240.1	3.711 x 10^{14} (kmol·Pa$^{(0.5)}$/kg$_{cat}$·s)
k_2	67.13	5.431 x 10^{-3} (kmol/kg$_{cat}$·s·Pa)
k_3	243.9	8.944 x 10^{13} (kmol·Pa$^{(0.5)}$/kg$_{cat}$·s)

Table 4: Heat of adsorption and pre-exponential factors for adsorption constant K_i

Adsorption Constant	Heat of adsorption ΔH_i (kJ/mol)	Pre-exponential factor A_i
K_{CO}	-70.65	8.23 x 10^{-4} (MPa)$^{-1}$
K_{CH_4}	-38.28	6.65 x 10^{-3} (MPa)$^{-1}$
K_{H_2O}	88.68	1.77 x 10^{5} (unit less)
K_{H_2}	-82.9	6.12 x 10^{-8} (MPa)$^{-1}$

Table 5: Equilibrium constant K_{pi}

Equilibrium constant K_{pi}	Units
K_{p1}=1.198 x 10^{11}*exp(-26830/T)	(MPa)^2
K_{p2}=1.77 x 10^{-2}*exp(4400/T)	(MPa)^0
$K_{p3} = K_{p1} \cdot K_{p2}$	(MPa)^2

The constants used in the current model for each of the chemical expressions of interest are presented in Table 3, Table 4 and Table 5, which are derived from literatures [42-44]. It is noteworthy that the above rate equations for the major reactions are dealing with intrinsic kinetics of methane-steam reforming and water-gas shift on the nickel based catalyst, and do not account for diffusion limitations. A more accurate reformer model needs to combine both reaction kinetics and diffusion limitations to have a more accurate prediction. However, the focus of current study is on the NH_3 conversion within reformer. NH_3 rate expressions as given in equations (10) and (12) were derived from experimental data, which accounted for diffusion effects.

4.3. SOFC stack

Detailed kinetic modeling of NH_3 reaction within SOFC stack is not considered in the current work. Instead, conversion ratio of NH_3 based on reference work is investigated and summarized as reference for consideration. A complete model of NH_3 reaction including consideration of chemical kinetics, mass transfer, and heat transfer will be built in the future.

4.4. Combustion zone

Mixing phenomena and reaction modes are shown in Figure 7, where depleted fuel from recirculation zone is mostly reacted in the area between SOFC tubes. Gas from that area is mixed and reacted with more air in the area between air feed tubes. SOFC tube has an external diameter of 2.2cm, while distance between SOFC tubes is about 3.3cm.

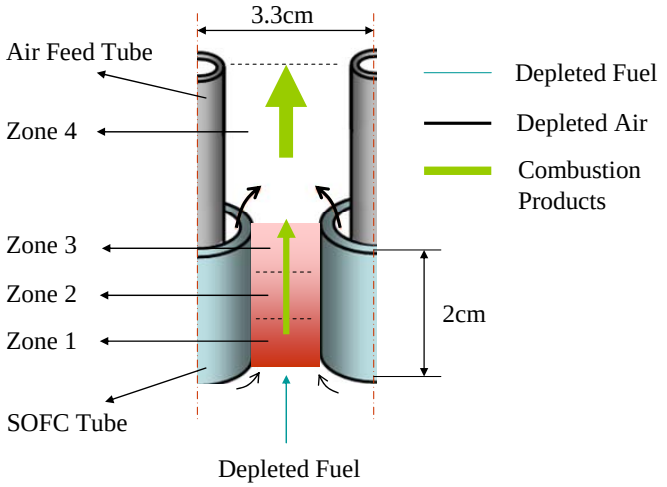

Figure 7: Mixing phenomena and modeling zones

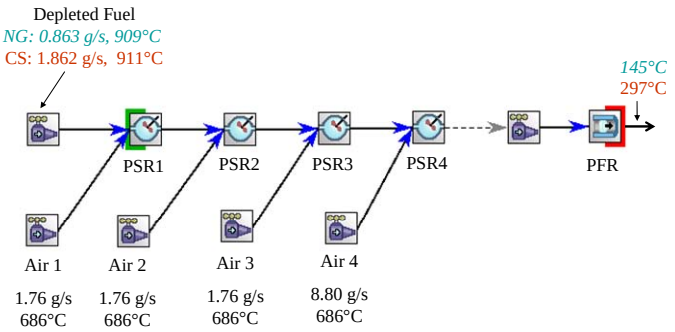

Figure 8: CHEMKIN model for combustion zone

A kinetic model for simulating the combustion zone was achieved using CHEMKIN 4.0.2 for both cases of natural gas and coal syngas (see Figure 8). Mass flow rates and temperatures for model inlets and outlet were predicted using APSAT simulation tool (See [2]). To approximate the mixing

phenomena when anode depleted fuel enters the combustion zone, a series of Perfectly Stirred Reactors (PSRs) with stepwise addition of air are considered. Major reaction zone between SOFC tubes is equally divided into three zones and simulated using three PSR models. Total residence time for those three reactors is about 0.1 second. Area between air feed tubes is simulated with another PSR, with a residence time about 0.5 second. The phenomena including gas composition change due to the heat exchange and temperature drop after combustion products leaving the combustion zone are simulated using a Plug Flow Reactor (PFR). Reaction mechanisms (GRI 3.0) are provided in CHEMKIN, which can predict potential fuel NO_x from NH_3 as well as thermal NO_x. PSR model is applied due to its simplicity and also because it provides solutions to flame problems more quickly [45].

5. RESULTS AND DISCUSSIONS

5.1. Preliminary equilibrium analysis

The equilibrium model from CHEMKIN 4.0.2, coupled with steady state analysis tool APSAT, was firstly used to estimate the gas composition after each of the three reacting components – reformer, SOFC stack and combustor. Typical coal syngas from Wabash coal gasification project is considered [1, 46]. Major results are summarized in the Table 6, which suggest:

a) Most of the NH_3 is cracked into N_2 and H_2 before entering combustion zone. In case of coal syngas containing 0.2% NH_3, only 13ppm NH_3 remains in the reformate stream and enters SOFC stack, while NH_3 conversion within the reformer is 99.2%. More NH_3 conversion is found in SOFC stack assuming chemical equilibrium is reached, which leaves only 0.3ppm NH_3 entering the combustion zone.

b) When comparing NO_x levels after the combustion zone with and without NH_3 contained in the fuel stream, it is found that NH_3 is not the major contributor to the significant amount of NO and NO_2 predicted at the combustor outlet. Due to the high conversion based on equilibrium analysis, very little NH_3 (0.3ppm) remains after reacting in the reformer and SOFC, and therefore generates negligible fuel NO_x at combustion zone. NO_x level after combustion zone is predicted to be lower in the coal gas case than natural gas case due to lower combustor temperature.

c) NO_x level (less than 0.02ppm) in the system exhaust obtained from the equilibrium analysis is much underestimated when it is compared to the observed data. NO_x emissions have never observed to be higher than 1ppm, but still higher than 0.1ppm in the exhaust of 25kW SOFC system based on natural gas fuel [35], which suggests that a more detailed analysis of combustion zone should be conducted. In this work, a kinetics model is set up for such a detailed study with consideration of mixing and reaction phenomena.

d) CHEMKIN equilibrium analysis of NH_3 reaction in the reformer can provide reference values but inaccurate results for actual NH_3 conversion due to the low NH_3 concentration and short residence time (<0.5 second). More detailed kinetics study is necessary, and the results are shown in the following section.

Table 6: Results from CHEMKIN equilibrium analysis

Stream	Fresh Fuel	Ref. in	Ref. out	Anode out	Comb. in	Comb. out	Exhaust	Comb. in	Comb. out	Exhaust	Comb. in	Comb. out	Exhaust
Stream No.	1[1]	3[1]	4[1]	5[1]	(6+8)[1]	9[1]		(6+8)[2]	9[2]		(6+8)[3]	9[3]	
H_2, %	34.80	30.15	28.89	4.38	0.38			0.38			0.78		
O_2, %					16.80	16.90	16.90	16.80	16.23	16.23	17.30	16.71	16.71
N_2, %	2.00	2.00	2.03	1.94	74.73	78.32	78.32	74.73	75.19	75.19	76.96	77.46	77.46
H_2O, %		4.90	8.01	32.02	2.81	3.40	3.40	2.81	3.27	3.27	2.99	3.85	3.85
CH_4, %	1.90	1.66	0.36	0.31	0.03			0.03			0.02		
CO, %	45.30	39.84	44.56	9.6	0.83			0.83			0.51		
CO_2, %	15.80	21.19	16.15	51.16	4.42	1.36	1.36	4.42	5.31	5.31	1.42	1.97	1.97
NH_3, %	0.20	0.169	0.0013	3ppm	0.3ppm								
NO, ppm						68.44	0.007		65.71	0.007		81.95	~0
NO_x(15%O_2), ppm						126	0.134		100	0.105		146	0.02
M, gram/s	4.86	6.17	6.17	8.81	79.07	79.07	79.07	79.07	79.07	79.07	73.84	73.84	73.84
T, °C	17	750	750	911	815	815	297	815	815	297	836	836	145
P, Bar	2.7	1.14	1.14	1.12	1.085	1.085	1.032	1.085	1.085	1.032	1.085	1.085	1.032

1: Combustion with NH_3 injection (Coal syngas case)
2: Combustion without NH_3 injection (Coal syngas case)
3: Combustion without NH_3 injection (Natural gas case)

5.2. Reformer: kinetics results

The performance of reformer in natural gas case with SOFC anode recirculation is first analyzed using the ASPEN reformer kinetics model (see Figure 9). Methane reformation and reverse water shift reaction reach equilibriums at a reformer length ~0.3 meter. Due to the high reformer operating temperature (750°C), a significant content of CO (~21%) remains when exiting the reformer.

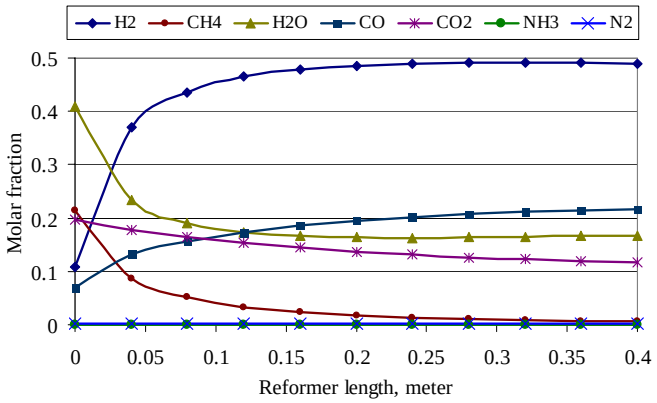

Figure 9: Reformer process stream profiles for natural gas

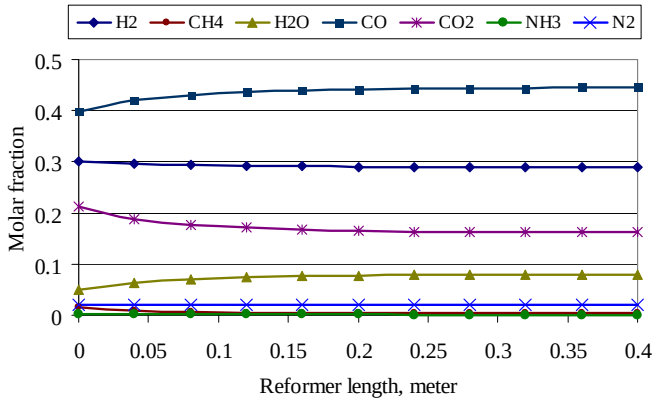

Figure 10: Reformer process stream profiles for coal syngas

Figure 10 shows the process stream profiles along the reactor obtained from the reformer kinetic model for coal syngas case. The reactions for major reactants (H_2, CO, CO_2, CH_4 and H_2O) reach thermodynamic equilibrium at a distance of 0.15 meter from the reformer inlet when mass transfer limitations are ignored. Due to low CH_4 content and high CO_2 content contained in the coal syngas, steam reforming is insignificant and the species concentrations are not changed much, which suggests that a reformer may not be necessary for just operating on typical coal syngas, unless the SOFC system is designed for multi-fuel (e.g., natural gas, biogas and coal syngas) operation, or coal syngas contains significant amounts of CH_4 as in the case of syngas from Lurgi or British Gas Lurgi (BGL) gasifiers. Instead, since CO content is very high (>40%) and water gas shift reaction is exothermic, a shift reactor may be considered to couple with SOFC stack when operating on coal syngas for converting CO into H_2 and provide some flexibility to help relieve the challenge of thermal management within SOFC stack.

Residence times for natural gas and coal syngas are compared in Figure 11. Due to the lower inlet flow rate (see Table 2), reformer on coal syngas show a smaller residence time at the beginning compared to natural gas. At the very end of the reformer, coal syngas case shows a higher residence time, because coal syngas composition doesn't change much along the reformer, however, molar flow rate keeps increasing in natural gas case when steam reformation occurs.

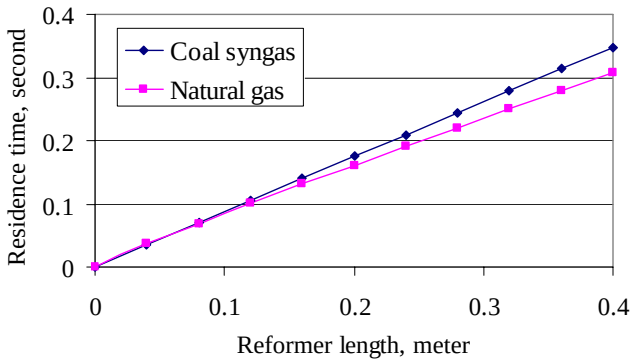

Figure 11: Residence time comparison

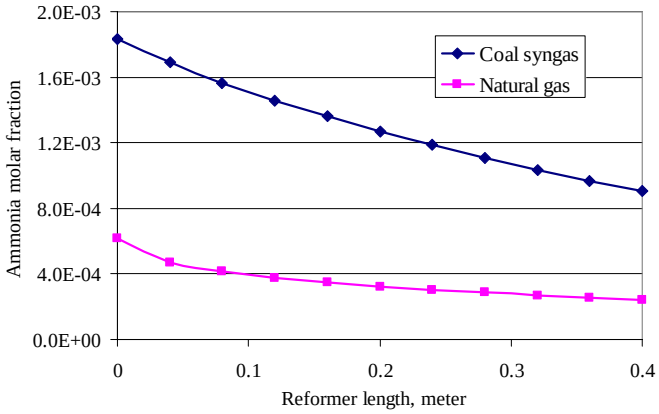

Figure 12: NH_3 conversion along the reformer

NH_3 reaction is considered and its conversion in the reformer is predicted based on the reaction mechanism and rate constant introduced in equations (10) and (12). For coal syngas case, as shown in Figure 12, the NH_3 reaction does not reach equilibrium within the reformer reactor, and the NH_3 conversion is limited to about 50% at the end of reformer (temperature = 750°C). For natural gas case, NH_3 reaction almost reaches equilibrium at the end of reformer due to its

lower inlet NH_3 content, which is highly diluted by the recirculated anode depleted fuel.

It is noteworthy that NH_3 conversion has a nearly linear dependence on the reformer operating temperature. The increase of temperature enhances the conversion (see Figure 13), because NH_3 decomposition is endothermic. When temperature is lowered to 700°C from 750°C, the NH_3 conversion within the reformer will decrease to 16% from 50% for coal syngas case, and from 45% to 15% for natural gas case.

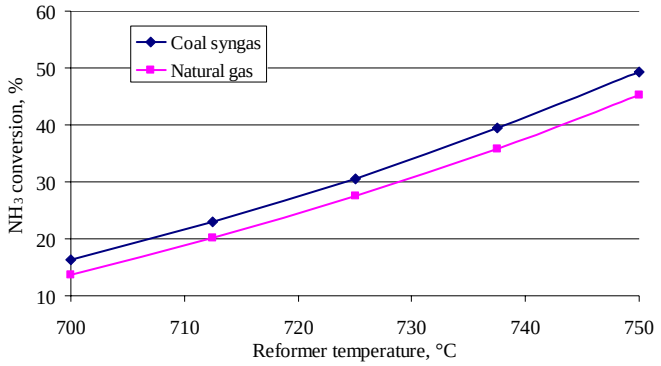

Figure 13: Dependence of NH_3 conversion on reformer temperature

Temkin-Pyzhev mechanism and rate constant based on equation (13) have also been incorporated into the reformer model, and the results show that NH_3 reaction reaches thermodynamic equilibrium very quickly (less than 0.0001 second). Considering equation (13) is derived at very high pressure, this fast reaction mechanism is not adapted in this work.

5.3. SOFC

As introduced before, an accurate prediction of NH_3 reactions and conversion in SOFC stack requires a comprehensive understanding of all different factors that could affect NH_3 reaction formats and rates, which could be very complicated and need a separate study. In this work, the following two assumptions are made for simplification based on the results shown in literature [10, 13, 19, 21]:

- All the reacted NH_3 is cracked into H_2 and N_2.
- NH_3 conversion (with the formation of N_2) is in the range of 80-99.996%.

5.4. Combustion zone

NO_x predictions from combustion zone model are summarized in Table 7, which are generated based on different cases with various fuel types, NH_3 contents and NH_3 conversions in SOFC stack. All NO_x values are adjusted to a 15% O_2 dry bases.

When typical natural gas is used as the fuel (case NG 1), thermal NO_x emissions are predicted to be about 0.3ppm which is close to the observed data of 0.35ppm [35]. When 0.2% NH_3 is added into natural gas (case NG 2), and 80% NH_3 conversion in the SOFC stack is assumed, then NO_x level is about 3.5ppm. Combustion zone in Case NG 2 has almost the same operating conditions (e.g., temperature, residence time…) as Case NG 1 due to the negligible effects of low content of NH_3. Therefore, the thermal NO_x emissions from Case NG 2 can be considered the same as in Case NG 1 – about 0.3ppm. The increased NO_x in Case NG 2, fuel NO_x, is sourced from the adding of NH_3. The conversion of NH_3 to NO_x in the combustion ozone is about 53% (see Table 8), where the left part of NH_3 is converted into N_2.

For coal syngas cases, thermal NO_x, as shown in case CS 1, is about 0.16ppm, lower than NG Case 1 due to the lower temperature. Fuel NO_x is found significantly depended on the NH_3 conversion in the reformer and SOFC stack. When NH_3 conversion in the reformer is about 50% as predicted by the model at a temperature of 750°C and the NH_3 conversion in SOFC is low (80%), 0.2% NH_3 contained in the coal syngas can cause 17ppm total NO_x for a SOFC system integrated with a reformer, and 37ppm NO_x without a reformer. Therefore, a reformer can help reduce NO_x emissions when NH_3 conversion is not very high at SOFC stack.

Table 7: NH_3 conversion and NO_x prediction

	NH_3 fraction				NO_x, ppm (15% O_2)
Cases	Fresh fuel	Reformer outlet	NH_3 conv. in SOFC, %	FC anode outlet	System exhaust
NG 1	0	0	N/A	0	0.3
NG 2	0.002	0.00024	80	0.000048	3.5
CS 1	0	0	N/A	0	0.16
CS 2	0.002	0.0009	80	0.00018	17
CS 3	0.002	N/A	80	0.0004	37
CS 4	0.002	0.0009	99.996	3.6E-08	0.16
CS 5	0.002	N/A	99.996	8.0E-08	0.17

Table 8: Analysis results for NH_3 to NO_x conversion

Cases	NG 2	CS 2
Comb. zone inlet NH_3, 10^{-6} mol/s	1.79	10.5
Comb. zone outlet NH_3, 10^{-6} mol/s	2.65×10^{-5}	1.68×10^{-4}
Total NO_x emissions, 10^{-6} mol/s	1.04	6.08
NO_x from NH_3, 10^{-6} mol/s	0.95	6.03
NH_3 to NO_x, %	53	57

When the conversion is high (99.996%), the NO_x emissions are very low (less than 0.2ppm) for each case, and concern about NH_3 as a contaminant in the coal syngas is not necessary. It suggests that coal syngas from high temperature coal gasifier can be directly sent to SOFC system without special design for NH_3 removal. Also, it suggests that if NH_3

conversion is high in SOFC stack, a reformer is not necessary for SOFC system to crack NH_3 when operating on such type of coal syngas.

The mechanism routes for NH_3 to form NO_x are plotted in Figure 14 for both cases of natural gas and coal syngas. NH_3 molecule is first broken down into NH_2 species. NH_2 is converted into NH or HNO via reactions with O or OH. NH reacts with O_2 or O to form NO directly, or is converted to HNO. HNO reacts with OH, O_2, O or H to form NO. NO is the only source for forming NO_2 and they can convert to each other. The net increase of NO_x (NO & NO_2) comes from either NH or HNO. Natural gas and coal syngas show similar reaction routes for NO_x generation from NH_3.

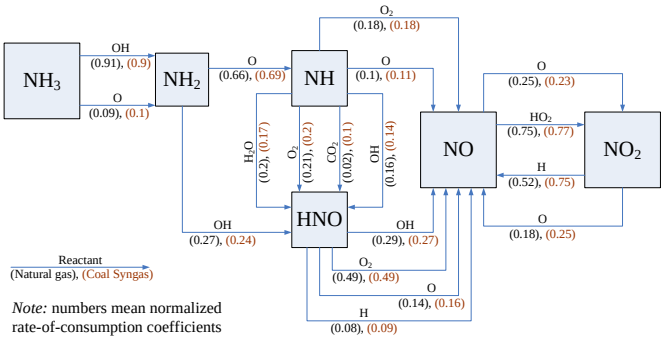

Figure 14: Mechanism analysis for NH_3 to NO_x conversion

Table 9: NO formation analysis (reactor PSR 1)

Cases	NG		CS	
Residence time	0.01	0.02	0.01	0.02
Reactor exit temperature, °C	1066	1165	1047	1129
NO net formation rate in each reaction, mol/m^3/s				
N+O2<=>NO+O		0.26		
HNO+O<=>NO+OH	0.73	0.53	4.8	3.8
HNO+H<=>H_2+NO	0.4	0.36	2.6	2.6
HNO+OH<=>NO+H_2O	1.5	2.0	8.2	11
HNO+O_2<=>HO_2+NO	2.5	2.3	15	13
NH+O_2<=>NO+OH	0.35	0.31	1.9	1.6
NH+O<=>NO+H	0.2	0.18		
Overall NO net formation rate, mol/m^3/s	5.8	5.9	33	33
From HNO, %	88.4	87	92.7	92.1
From NH, %	9.5	8.2	5.8	4.8
Others, %	2.1	4.4	1.5	3.1

It is also noteworthy that the NO_x reduction mechanism as introduced in equation (19) is insignificant in this combustion zone due to the high local temperature in this study. For both cases of natural gas and coal syngas, the temperatures in different PSRs are higher than 860°C (higher ~1100°C in PSR 1 for both cases of natural gas and coal syngas as seen in Table 9), which is out of the temperature window (750-850°C) for the SNCR reaction to occur.

Quantitative analysis of NO formation in different routes is conducted and the results are summarized in Table 9. Because NO_2 comes from NO, the formation rate analysis of NO is equivalent to NO_x. It is found that most of NO is produced in the first PSR reactor (PSR 1). The NO formations in the other PSR reactors are at least 2 orders of magnitude less than PSR 1. Thus, the analysis is focused on PSR 1. For both of natural gas and coal syngas cases, about 90% NO is formed from HNO and the left is mainly from NH. In PSR 1, the residence time is about 0.02 second. Sensitivity analysis shows that the change of residence time affects the net formation rate in each reaction, but doesn't change much the overall NO net formation rate.

6. CONCLUSIONS

The study of this work suggests the following major conclusions:

1. NH_3 as a contaminant in the SOFC integrated system will not degrade SOFC performance based on literature review, however, potentially causes NO_x emissions from combustion zone according to the investigation in this work.
2. NH_3 conversion in the internal reformer is about 50% when temperature is 750°C based on model results.
3. More accurate theoretical understanding and prediction of NH_3 conversion in the SOFC stack need a comprehensive study of mass transfer, heat transfer chemical reactions and electrochemical reactions, which should consider the following major factors: catalyst, temperature, O^{2-} diffusivity and NH_3 diffusivity, residence time and NH_3 molar flow rate.
4. NH_3 conversion (into N_2 and H_2) in the SOFC stack can affect NO_x emissions significantly. The current study shows that when the conversion is high (99.996%) as some research groups suggested, the concern about NO_x emissions (less than 0.2 ppm) from NH_3 in the coal syngas is not necessary. It suggests that coal syngas may be directly sent to SOFC system without a reformer.
5. Lower NH_3 conversion in the SOFC stack may cause high fuel NO_x. When the conversion is 80%, 0.2% NH_3 contained in the coal syngas can generate 17 ppm NO_x with a reformer, and 37 ppm NO_x without a reformer.
6. More than 50% NH_3 left from SOFC stack, either natural gas case or coal syngas case, can convert into NO_x mainly (~90%) from the following formation route: $NH_3 \rightarrow NH_2 \rightarrow (NH) \rightarrow HNO \rightarrow NO(\leftrightarrow NO_2)$
7. SOFC system is promising to operate directly on coal syngas without special design on NH_3 removal.
8. An external or internal reformer is not necessary for SOFC system to operate on typical coal syngas, except for some special cases where coal syngas contains significant amounts of CH_4. But a reformer can be helpful for

cracking NH_3 and reducing NO_x emissions when NH_3 conversion in SOFC stack is not high enough.

9. A shift reactor may be considered to couple with SOFC stack when operating on coal syngas for converting CO into H_2 and provide some flexibility to help relieve the challenge of thermal management within SOFC stack.

ACKNOWLEDGMENTS

We acknowledge and appreciate the support of Southern California Edison, Siemens Westinghouse Power Corporation, and the California Energy Commission in the preparation of this paper.

REFERENCES

[1] *Fuel Cell Handbook*. Fifth ed. 2000: NETL, U.S. Department of Energy. 9-77.

[2] Y. Yi, A.D. Rao, J. Brouwer and G.S. Samuelsen, *Fuel flexibility study of an integrated 25 kW SOFC reformer system.* Journal of Power Sources, 2005. **144**(1): p. 67-76.

[3] *Wabash River Coal Gasification Repowering Project.* 2000, Wabash River Energy Ltd. p. 4-80.

[4] L.P. Harris and R.P. Shah, *Advanced Energy Conversion Systems-Conceptual Designs*. 1976.

[5] *Tampa Electric Polk Power Station Integrated Gasification Combined Cycle Project*. 2002, NETL, The U.S. Department of Energy: Morgantown, West Virginia. p. 260.

[6] K. Jothimurugesan, K and S.K. Gangwal. *Advances in Ammonia Removal from Hot Coal Gas*. in *Advanced Coal-Fired Power Systems '96 Review Meeting*. 1996.

[7] G.N. Krishnan, B.J. Wood, G.T. Tong and J.G. McCarty, *Study of Ammonia Removal in Coal Gasification Processes*. 1988, U.S. DOE/METC.

[8] W. Wang and G. Olofsson. *Reduction of Ammonia and Tar in Pressurized Biomass Gasification*. in *5th International Symposium on Gas Cleaning at High Temperature*. 2002. Morgantown, WV: NETL.

[9] P. Glarborg, A.D. Jensen, and J.E. Johnson, *Fuel nitrogen conversion in solid fuel fired systems.* Progress in Energy and Combustion Science, 2003. **29**.

[10] N. Dekker and B. Rietveld. *Highly efficient conversion of ammonia in electricity by solid oxide fuel cells*. in *6th European Solid Oxide Fuel Cell Forum*. 2004. Lucerne, Switserland.

[11] A. McFarlan, L. Pelletier, and N. Maffei, *An Intermediate-Temperature Ammonia Fuel Cell Using Gd-Doped Barium Cerate Electrolyte.* Journal of the Electrochemical Society, 2004. **151**(6).

[12] R.D. Farr and C.G. Vayenas, *Ammonia High Temperature Solid Electrolyte Fuel Cell.* Journal of the Electrochemical Society, 1980. **127**(7).

[13] J. Staniforth and R.M. Ormerod, *Clean destruction of waste ammonia with consummate production of electrical power within a solid oxide fuel cell system.* Green Chemistry, 2003. **5**(5): p. 606-609.

[14] A. Wojcik, H. Middleton, I. Damopoulos and J. Van Herle, *Ammonia as a fuel in solid oxide fuel cells.* Journal of Power Sources, 2003. **118**(1-2): p. 342-348.

[15] C.G. Vayenas and R.D. Farr, *Cogeneration of Electric Energy and Nitric Oxide.* Science, 1980. **208**(4444): p. 593-594.

[16] T.V. Choudhary, C. Sivadinarayana, and D.W. Goodman, *Catalytic ammonia decomposition: COx-free hydrogen production for fuel cell applications.* Catalysis Letters, 2001. **72**(3-4): p. 197-201.

[17] S. Stolbov and T.S. Rahman, *First Principles Study of Adsorption, Diffusion and Dissociation of NH3 on Ni and Pd Surfaces.* 2001.

[18] *Ammonia Crackers / Ammonia Cracking Units*. VAAVU Tech Engineering, 2005.

[19] A.S. Chellappa, C.M. Fischer, and W.J. Thomson, *Ammonia decomposition kinetics over Ni-Pt/Al2O3 for PEM fuel cell applications.* Applied Catalysis A: General, 2002. **227**(1-2): p. 231-240.

[20] M.R. Powell, M.S. Fountain, and C.J. Call. *Ammonia-based hydrogen generation for fuel cell power supplies.* 2002 [cited.

[21] R.W. McCabe, *Kinetics of ammonia decomposition on nickel.* Journal of Catalysis, 1983. **79**(2): p. 445-450.

[22] *Ammonia Cracking Units* 2005, M/s. AIROX NIGEN EQUIPMENTS PVT. LTD.

[23] J.C. Ganley, F.S. Thomas, E.G. Seebauer and R. I. Masel, *A Priori Catalytic Activity Correlations: The Difficult Case of Hydrogen Production from Ammonia.* Catalysis Letters, 2004. **96**(3 - 4): p. 117-122.

[24] J.J. Vajo, W. Tsai, and W.H. Weinberg, *Mechanistic details of the heterogeneous decomposition of ammonia on platinum.* Journal of Physical Chemistry 1985. **89**(15): p. 3243 - 3251.

[25] E.N. Gobina, J.S. Oklany, and R. Hughes, *Elimination of Ammonia from Coal Gasification Streams by Using a Catalytic Membrane Reactor.* Industrial & Engineering Chemistry Research, 1995. **34**: p. 3777 - 3783.

[26] M.E.E. Abashar, Y.S. Al-Sughair, and I.S. Al-Mutaz, *Investigation of low temperature decomposition of ammonia using spatially patterned catalytic membrane reactors.* Applied Catalysis A: General, 2002. **236**(1-2): p. 35-53.

[27] J.P. Collins, J.D. Way, and N. Kraisuwansarn, *A mathematical model of a catalytic membrane reactor for the decomposition of NH3.* Journal of Membrane Science, 1993. **77**(2-3): p. 265-282.

[28] J.P. Collins, *Catalytic decomposition of ammonia in a high temperature membrane reactor*, in *Journal of Membrane Science*. 1993, Oregon State University.

[29] G. Djega-Mariadassou, C.-H. Shin and G. Bugli, *Tamaru's model for ammonia decomposition over titanium oxynitride.* Journal of Molecular Catalysis A: Chemical,

1999. **141**(1-3): p. 263-267.
[30] S.T. Oyama, *Kinetics of ammonia decomposition on vanadium nitride*. Journal of Catalysis, 1992. **133**(2): p. 358-369.
[31] G. Papapolymerou and V. Bontozoglou, *Decomposition of NH3 on Pd and Ir Comparison with Pt and Rh.* Journal of Molecular Catalysis A: Chemical, 1997. **120**(1-3): p. 165-171.
[32] N.J. Maskalisk and E.R. Ray. *Contaminant effects in solid oxide fuel cells*. in *The US DOE Contractors Review Meeting on Fuel Cells*. 1992. Morgantown, WV: Westinghouse Electric Corp.
[33] T.R. Fabis and L.A. Shockling, *Operation manual for ARPA/SCE 27kWe AES SOFC generator system*. 1995, Westinghouse STC: Pittsburgh, Pennsylvania. p. 6.
[34] H.S. Fogler, *Elements of Chemical Reaction Engineering*. 3 ed. Prentice Hall International Series in the Physical and Chemical Engineering Sciences, ed. N.R. Amundson. 1999, Englewood Cliffs, New Jersey: Prentice Hall PTR.
[35] W.J. Skrivan, *Parametric testing and analysis of a 25kW SOFC system*, in *Department of Mechanial and Aerospace Engineering*. 2002, University of California: Irvine.
[36] L. Lietti, C. Ramella, G. Groppi and P. Forzatti, *Oxidation of NH3 and NOx formation During the catalytic combustion of gasified biomasses fuels over Mn-hexaaluminate and alumina-supported Pd catalysts.* Applied Catalysis B: Environmental, 1999. **21**(2): p. 89-101.
[37] Y. Lu, I. Hippinen, and A. Jahkola, *Control of NOx and N2O in pressurized fluidized-bed combustion.* Fuel, 1995. **74**(3): p. 317-322.
[38] Y. Yi, T.P. Smith, J. Brouwer, A.D. Rao and G.S. Samuelsen, *Simulation of A 220 KW Hybrid SOFC Gas Turbine System and Data Comparison*. in *Eighth International Symposium on Solid Oxide Fuel Cell (SOFC-VIII)*. 2002. Paris, France.
[39] A.D. Rao and G.S. Samuelsen, *Analysis Strategies for Tubular Solid Oxide Fuel Cell Based Hybrid Systems.* Journal of Engineering for Gas Turbines and Power, 2002. **124**: p. 503-509.
[40] S.C. Smugeresky, *Transient Modeling of a Tubular Solid Oxide Fuel Cell System*, in *Mechanical and Aerospace Engineering*. 2003, University of California: Irvine.
[41] F. Mueller, *Design and simulation of a tubular solid oxide fuel cell system control strategy*, in *Mechanical and Aerospace Engineering*. 2005, University of California: Irvine. p. 160.
[42] J. Xu and G.F. Froment, *Methane Steam Reforming: II. Diffusional Limitations and Reactor Simulation.* AIChE Journal, 1989. **35**(1): p. 97-103.
[43] J. Xu and G.F. Froment, *Methane Steam Reforming, Methanation and Water-Gas Shift: I. Instrinsic Kinetics.* AIChE Journal, 1989. **35**(1): p. 88-96.
[44] K. Hou and R. Hughes, *The kinetics of methane steam reforming over a Ni/[alpha]-Al2O catalyst.* Chemical Engineering Journal, 2001. **82**(1-3): p. 311-328.
[45] H.P. Mallampalli, T.H. Fletcher, and J.Y. Chen. *Evaluation of CH4/NOx Global Mechanisms Used for Modeling Lean Premixed Turbulent Combustion of Natural Gas*. in *The Fall Meeting of the Western States Section of the Combustion Institute University of Southern California*. 1996. Los Angeles, CA.
[46] *Wabash River Coal Gasification*. 2000, NETL, The U.S. Department of Energy: Wabash River Energy Ltd., Morgantown, West Virginia. p. 358.